### **MJSAT**

### Malaysian Journal of Science and Advanced Technology

MALAYSIAN JOURNAL
OF SCIENCE AND
ADVANCED
TECHNOLOGY
LINE AND ADVANCED
TECHNOLOGY
LINE AND ADVANCED
TECHNOLOGY
LINE AND ADVANCED
TECHNOLOGY
LINE AND ADVANCED
TECHNOLOGY
LINE AND ADVANCED
TECHNOLOGY
LINE AND ADVANCED
TECHNOLOGY
LINE AND ADVANCED
TECHNOLOGY
LINE AND ADVANCED
TECHNOLOGY
LINE AND ADVANCED
TECHNOLOGY
LINE AND ADVANCED
TECHNOLOGY
LINE AND ADVANCED
TECHNOLOGY
LINE AND ADVANCED
TECHNOLOGY
LINE AND ADVANCED
TECHNOLOGY
LINE AND ADVANCED
TECHNOLOGY
LINE AND ADVANCED
TECHNOLOGY
LINE AND ADVANCED
TECHNOLOGY
LINE AND ADVANCED
TECHNOLOGY
LINE AND ADVANCED
TECHNOLOGY
LINE AND ADVANCED
TECHNOLOGY
LINE AND ADVANCED
TECHNOLOGY
LINE AND ADVANCED
TECHNOLOGY
LINE AND ADVANCED
TECHNOLOGY
LINE AND ADVANCED
TECHNOLOGY
LINE AND ADVANCED
TECHNOLOGY
LINE AND ADVANCED
TECHNOLOGY
LINE AND ADVANCED
TECHNOLOGY
LINE AND ADVANCED
TECHNOLOGY
LINE AND ADVANCED
TECHNOLOGY
LINE AND ADVANCED
TECHNOLOGY
LINE AND ADVANCED
TECHNOLOGY
LINE AND ADVANCED
TECHNOLOGY
LINE AND ADVANCED
TECHNOLOGY
LINE AND ADVANCED
TECHNOLOGY
LINE AND ADVANCED
TECHNOLOGY
LINE AND ADVANCED
TECHNOLOGY
LINE AND ADVANCED
TECHNOLOGY
LINE AND ADVANCED
TECHNOLOGY
LINE AND ADVANCED
TECHNOLOGY
LINE AND ADVANCED
TECHNOLOGY
LINE AND ADVANCED
TECHNOLOGY
LINE AND ADVANCED
TECHNOLOGY
LINE AND ADVANCED
TECHNOLOGY
LINE AND ADVANCED
TECHNOLOGY
LINE AND ADVANCED
TECHNOLOGY
LINE AND ADVANCED
TECHNOLOGY
LINE AND ADVANCED
TECHNOLOGY
LINE AND ADVANCED
TECHNOLOGY
LINE AND ADVANCED
TECHNOLOGY
LINE AND ADVANCED
TECHNOLOGY
LINE AND ADVANCED
TECHNOLOGY
LINE AND ADVANCED
TECHNOLOGY
LINE AND ADVANCED
TECHNOLOGY
LINE AND ADVANCED
TECHNOLOGY
LINE AND ADVANCED
TECHNOLOGY
LINE AND ADVANCED
TECHNOLOGY
LINE AND ADVANCED
TECHNOLOGY
LINE AND ADVANCED
TECHNOLOGY
LINE AND ADVANCED
TECHNOLOGY
LINE AND ADVANCED
TECHNOLOGY
LINE AND ADVANCED
TECHNOLOGY
LINE AND ADVANCED
TECHNOLOGY
LINE AND ADVANCED
TECHNOLOGY
LINE AND ADVANCED
TECHNOLOGY
LINE AND ADVANCED
TECHNOLOGY
LINE AND ADVANCED
TECHNOLOGY
LINE AND ADVANCED
TECHNOLOGY
LINE AND ADVANCED
TECHNOLOGY
LINE AND ADVANCED
TECHNOLOGY
LINE AND ADVANCED
TEC

journal homepage: <a href="https://mjsat.com.my/">https://mjsat.com.my/</a>

# Application of Geostatistical Kriging Model in Assessing Exposure to Background Ionizing Radiation and its Radiological Hazard Indices

Sijibomi O. Awokoya<sup>1</sup>, Paul S. Ayanlola<sup>1\*</sup>, Adewale Olatunji<sup>2</sup>, Festus A. Ojeniyi<sup>1</sup>, Omololu I. Agbelusi<sup>1</sup>, Olalere T. Orodiran<sup>1</sup>, and Gbadebo A. Isola<sup>1</sup>

### **KEYWORDS**

Background ionizing radiation Geostatistics Kriging model Radiological indices

### **ARTICLE HISTORY**

Received 10 September 2024 Received in revised form 1 October 2024 Accepted 31 October 2024 Available online 1 November 2024

### **ABSTRACT**

Background ionizing radiation from natural sources is a pervasive environmental factor that poses significant health risks. Rural assessment of developing nations is often neglected, due to perceived lower radiation risk and limited industrialization. This study therefore addresses this gap by measuring the terrestrial gamma dose rates, estimate the radiological hazards, and predict the gamma dose rates at unobserved locations using Kriging Model in Ogbomoso South Local Government, a rural region within Oyo State, Nigeria. A systematic random sampling was conducted within 10 administrative wards. Insitu gamma dose rate measurements were taken using a Radex, RD 1503 dosimeter and ArcMap was used to generate spatial map. Terrestrial average gamma dose rates (ADR) ranging from 0.122 to 0.139 μSvh<sup>-1</sup>, with an overall average of 0.132 μSvh<sup>-1</sup>, which is below the global average of 0.274 µSvh<sup>-1</sup>. The estimated annual effective dose equivalent ranged from 0.213 to 0.243 mSvy<sup>-1</sup>, averaging 0.231 mSvy<sup>-1</sup>, significantly below permissible limits of 1 mSvy<sup>-1</sup>. The spatial map of ADR distribution, ranged from 0.085 to 0.179 µSvh<sup>-1</sup>. The study concludes that current radiation exposure level poses no significant radiological hazard. It recommends regular monitoring program to track changes over time with the data considered as baseline for Ogbomoso South local Government.

 $\hbox{@}$  2024 The Authors. Published by Penteract Technology.

This is an open access article under the CC BY-NC 4.0 license (https://creativecommons.org/licenses/by-nc/4.0/).

### 1. Introduction

Natural radioactive sources present in soil, water, and air ubiquitously emit ionizing radiation autonomously, thus impacting various environmental materials and processes without human intervention. Among these sources is Naturally Occurring Radioactive Material (NORM), which comprises primordial radionuclides like uranium, thorium, potassium, and their decay products such as radium and radon [1]. These radionuclides, with their unstable atomic nuclei, release radiation energy as they stabilize, thereby permeating various ecological and geographical strata and influencing the environment in multiple ways [2].

Gamma radiation, a product of both the natural decay of primordial radionuclides and cosmic rays, is a major form of ionizing radiation exposure to the human body. This highenergy radiation contributes significantly to background radiation levels and can penetrate deeply into biological tissues, disrupting cellular structures and leading to potential health risks, including cancer after prolonged exposure [3]. Furthermore, human activities such as mining, medical practices, and nuclear power generation exacerbate exposure to ionizing radiation [4], making background ionizing radiation (BIR) a crucial environmental factor with significant health implications.

A review of previous studies reveals that radiation exposure assessments have been extensively conducted in both urban and rural settings, focusing on the health risks posed by background ionizing radiation. Studies by [5] and [6] have provided global estimates of radiation exposure, highlighting the contribution of natural sources to the overall radiation burden on the population. Recent work by [7] and [8] has contributed significantly to understanding radiation exposure

E-mail address: Paul S. Ayanlola < psayanlola 28@lautech.edu.ng>.

https://doi.org/10.56532/mjsat.v4i4.381

2785-8901/© 2024 The Authors. Published by Penteract Technology.

<sup>&</sup>lt;sup>1</sup>Department of Pure and Applied Physics, Ladoke Akintola University of Technology, Ogbomoso, Nigeria.

<sup>&</sup>lt;sup>2</sup>Department of Physics, Ajayi Crowther University, Oyo, Nigeria.

<sup>\*</sup>Corresponding author:

in Nigeria, particularly in regions with varying geological characteristics. These studies underscore the importance of local geology, such as the presence of granite and sedimentary rock formations, which are rich in uranium and thorium, leading to elevated radiation levels.

In rural regions, where environmental monitoring is often limited because of the geographical isolation [9], there is an increasing need to apply geostatistical models to accurately map radiation levels. Kriging has emerged as one of the most widely used models in radiation exposure assessments due to its ability to interpolate radiation levels in unobserved locations [10, 11]. Studies by [12, 13] have applied Kriging to map radiation exposure in various parts of Europe and Africa, respectively, demonstrating the model's versatility across diverse environments. These studies show that factors like soil composition, rock types, and land use patterns significantly influence spatial radiation distribution, making geostatistical models essential for comprehensive assessments.

Other geostatistical tools such as the Co-Kriging and Inverse Distance Weighting (IDW) have also been used effectively to predict radiation levels in complex terrains [14, 15]. [16] highlight the advantages of Co-Kriging in incorporating auxiliary variables, such as elevation or soil properties, to improve the precision of radiation exposure maps. Moreover, studies by [14, 17] have successfully applied IDW in areas with sparse sampling data, showing that it can provide reliable results when Kriging data are insufficient or unreliable. These methods further demonstrate the importance of selecting appropriate geostatistical tools based on the characteristics of the study area.

In Nigeria, previous research has utilized geostatistical models to assess radiation exposure, particularly in urban and industrial areas. [18, 19] explored the spatial distribution of gamma radiation in both densely populated and rural settings, linking variations in radiation levels to geological factors and human activities like mining and agriculture. However, rural areas remain understudied, and comprehensive ecoradiological baselines for regions like Ogbomoso South Local Government are lacking. This study seeks to address this gap by applying the Kriging model to estimate the gamma dose rates in Ogbomoso South, thereby providing a spatially detailed analysis of BIR levels, facilitating targeted assessments and interventions to mitigate potential health risks and help the policymakers to assess radiation risks and develop mitigation strategies [20].

### 2. MATERIALS AND METHODS

### 2.1 Study area

The study was conducted in Ogbomoso South Local Government, Oyo State, Nigeria. This area, located in the southwestern region of the country, lies between latitude 8°13'0" N and longitude 4°15'0" E, covering approximately 88 km². The study area includes 10 administrative wards which are: Akata, Alapata, Arowomole, Ibapon, Ijeru I, Ijeru II, Isoko, Ilogbo, Lagbedu, and Oke-Ola/Farm Settlement. These wards were selected due to their distinct geological formations and the variety of economic activities present, such as agriculture, artisanal textile production, and welding, all of which may contribute to the presence and distribution of naturally occurring radioactive materials (NORMs). The

choice of Ogbomoso South Local Government as the study area is further justified by its ecological diversity comprising soil, water, and vegetation each of which can influence the accumulation and distribution of radiation. Figure 1 presents a map of the study area, generated using ArcMap (Version 10.8.2).

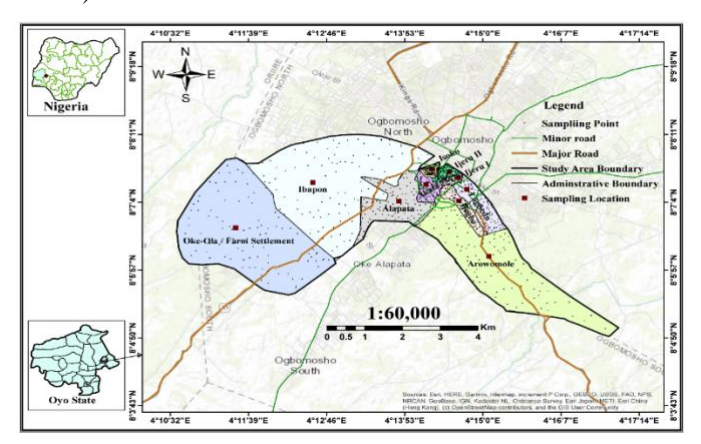


Fig. 1. Map of the study area, indicating the sampling locations

### 2.2 Materials

The following materials were used for data collection and analysis: a Global Positioning System (GPS) device, which was used to accurately record the geographic coordinates of each sampling point; a portable dosimeter (Radex RD 1503) equipped with a Geiger-Muller tube to measure levels of background ionizing radiation (BIR) at each sampling site; ArcMap (Version 10.8.2) for spatial analysis and the generation of spatial distribution maps; and Microsoft Excel for processing and conducting descriptive analysis of the collected data.

### 2.3 Sampling techniques

A total of 1,000 radiation measurements were taken from 100 locations across the 10 administrative wards, ensuring even spatial distribution across the study area. At each location, measurements were taken randomly at 5-meter intervals to achieve comprehensive coverage and minimize spatial bias. This interval was chosen to balance the need for detailed spatial resolution with the practical constraints of fieldwork. GPS coordinates were recorded for each point, followed by in-situ BIR measurements using the Radex RD 1503 dosimeter. Each location was measured twice, and the average reading was recorded to increase the reliability of the data.

### 2.4 Description of the dosimeter

The Radex RD 1503, version 10.KP.01.00.00.000 is a portable dosimeter featuring a Geiger-Muller detector tube, capable of detecting both gamma and beta radiation. The device operates within a temperature range of -10°C to 50°C, with a sensitivity range starting from 10 keV through its detection window and 40 keV through its casing. It can operate in relative humidity levels of up to 80% at 25°C. The dosimeter displays radiation levels in  $\mu Svh^{-1}$  or  $\mu Remh^{-1}$ , making it suitable for environmental radiation assessments. Given its user-friendly design and built-in self-calibration, the Radex RD 1503 was well-suited for field measurements in the study area.

### 2.5 Background radiation measurement

At each sampling site, the dosimeter was held 1 meter above ground level and rotated 360 degrees to capture an averaged background radiation reading. The device was allowed to complete an initial 10-second observation cycle before it commenced a series of 10-second measurement cycles. The average reading from these cycles, recorded after 40 seconds, was logged, and later digitized for further analysis. This procedure was repeated consistently across all measurement points to ensure data uniformity. Average gamma dose rates (ADR) were then calculated using Microsoft Excel for subsequent spatial analysis.

# 2.6 Determination of radiological parameters and Kriging Interpolation for Gamma Dose Rate Estimation

### 2.6.1 Annual effective dose equivalent

The annual effective dose equivalent (AEDE), which quantifies the radiation dose absorbed by individuals in the study area, was calculated following the standard model described by [21, 22] in equation 1. The calculation converts the recorded average gamma dose rates into an annual dose that reflects potential human exposure.

$$AEDE\ (mSvy^{-1}) = ADR \times 8760 \times 0.2 \times 10^{-3}$$
 (1)

where ADR is the average Gamma dose rate in  $\mu$ Svh<sup>-1</sup>, 0.2 is the outdoor occupancy factor, 8760 hy<sup>-1</sup> is the conversion factor from hours to year,  $10^{-3}$  is the conversion factor from  $\mu$ Svhr<sup>-1</sup> to mSvhr<sup>-1</sup>.

### 2.7 Kriging interpolation for gamma dose rate prediction

Kriging, a geostatistical method, was used to estimate gamma dose rates at unobserved locations based on data from measured points. Geospatial analysis was conducted in ArcMap 10.8.2 using the Spatial Analyst extension in the Geographic Information System (GIS) environment where Kriging interpolation process was implemented, and spatial Map generated.

Prior to applying the Kriging method, the measured data collected was tested for normality using histograms tool in ArcMap, which provided results for skewness and kurtosis to ensure the data met the necessary assumptions for accurate spatial interpolation. Data was then processed following the standard Kriging procedure, which includes semivariogram creation, model fitting, and the calculation of spatial weights as illustrated in Figure 2.

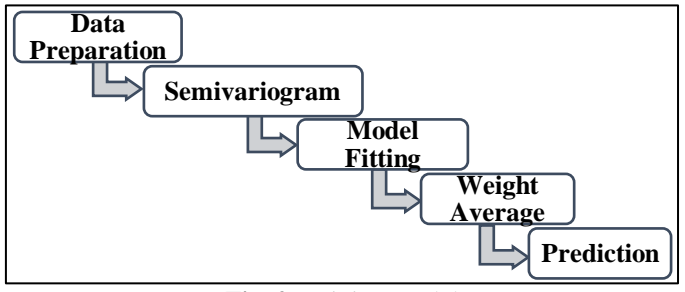


Fig. 2. Kriging model

A semivariogram was generated to examine the spatial autocorrelation of the measured data points. Theoretical model was fitted to the semivariogram to describe spatial continuity, ensuring that data from neighbouring points were appropriately weighted during interpolation. Weighted averages of the data were calculated using the fitted model, allowing for spatial prediction of gamma dose rates at unobserved locations.

### 2.8 Kriging formulation

The Kriging formulation as presented by [23, 24], is shown in equation (2)

$$\widehat{Z}(S_0) = \sum_{i=1}^n \lambda_i Z(S_i)$$
 (2)

where  $\widehat{\mathbf{Z}}(S_0)$  represents the estimated value at unobserved location  $S_0$ ,  $\lambda_i$  is Kriging weight assigned to measured values  $Z(S_i)$  at location  $S_i$ . These weights are determined based on spatial configuration of the spatial points and the spatial correlation structure (semivariogram). The sum of the weight  $\lambda_i$  equals 1, **n** is the number of measured locations used to estimate the value at  $S_0$ . The Kriging interpolation technique was implemented by transferring the average dose rates (ADR) data into a Geographic Information System (GIS) environment. The data was processed within the Spatial Analyst extension module in ArcMap 10.8.2 software, where comprehensive spatial analysis was performed using prepared maps. An experimental semivariogram analysis was conducted to assess how spatial variability changes with distance and direction, which is crucial for determining the reliability of the generated maps.

#### 2.9 Model validation metrics

The accuracy of the Kriging model was assessed through post-validation metrics such as the Mean Error (ME), Root Mean Square Error (RMSE), Mean Standardized Error (MSE), Root Mean Square Standardized Error (RMSSE), and Average Standard Error (ASE) to validate the model's accuracy and reliability to produce spatial predictions.

The formulas for these metrics are expressed in equation (3) to (7)

ME = 
$$\frac{1}{n} \sum_{i=1}^{n} [Z(S_i) - \hat{Z}(S_i)]$$
 (3)

MSE = 
$$\frac{1}{n} \sum_{i=1}^{n} [Z(S_i) - \widehat{Z}(S_i)]^2$$
 (4)

RMSE = 
$$\sqrt{\frac{1}{n} \sum_{i=1}^{n} [Z(S_i) - \hat{Z}(S_i)]}$$
 (5)

RMSSE = 
$$\sqrt{\frac{1}{n} \sum_{i=1}^{n} \left[ \frac{Z(S_i) - \widehat{Z}(S_i)}{\sigma(S_i)} \right]}$$
 (6)

ASE 
$$= \frac{1}{n} \sum_{i=1}^{n} \sigma(S_i) n$$
 (7)

The ME and RMSE in Equation 2.1 and 2.2 offer insights into the model's bias and accuracy, respectively. An ME close to 0 indicates minimal bias in the model's predictions and a low RMSE value signifies high accuracy [23, 24]. The MSE, RMSSE, and ASE in Equation 2.3 to 2.5 assess the calibration of the model's uncertainty estimates [25]. An MSE near zero indicates that the prediction errors are centered around the mean values [26]. RMSE and ASE values that are reasonably close, along with an RMSSE value near 1, signifies that the

model's predictions are well-scaled and reliable in evaluating performance [23,27]. Additionally, spatial visualization techniques like residual plot were used to further analyze the differences between predicted (estimated) and measured ADR values.

### 3. RESULTS

### 3.1 Gamma dose rate and annual effective dose equivalent

The results of in-situ measurements of background ionizing radiation in Ogbomoso South Local Government yielded a comprehensive dataset of 1,000 readings, as summarized in Table 1. The results reveal the average gamma dose rate (ADR) and estimated annual effective dose equivalent (AEDE) for the study area. The ADR ranged from 0.122 to 0.139  $\mu Svh^{-1}$ , with an overall average of 0.132  $\mu Svh^{-1}$ . The estimated AEDE values ranged from 0.213 to 0.243 mSvy<sup>-1</sup>, with an average of 0.231 mSvy<sup>-1</sup>

**Table 1.** Gamma dose rate and annual effective dose equivalent

Location	ADR (μSvh <sup>-1</sup> )	AEDE (mSvy <sup>-1</sup> )
Ijeru I	$0.122 \pm 0.00$	0.213
Ibapon	$0.128 \pm 0.01$	0.224
Isoko	$0.130\pm0.00$	0.228
Ilogbo	$0.130\pm0.00$	0.229
Lagbedu	$0.131 \pm 0.01$	0.230
Alapata	$0.131\pm0.02$	0.230
Arowomole	$0.136 \pm 0.01$	0.238
Akata	$0.136\pm0.00$	0.239
Ijeru II	$0.136 \pm 0.00$	0.239
Oke-Ola	$0.139 \pm 0.00$	0.243
Average	$0.132 \pm 0.00$	0.231

## 3.2 Kriging metric report and spatial map of the predicted gamma dose date

The results of kriging metrics report of the model's accuracy are presented in Table 2. The graphical representations of the normality test of ADR data using histogram tool in ArcMap, kriging semivariogram analysis, residual plot, and spatial map of predicted average gamma dose rates (ADR) are presented in Figure 3, 4, 5 and 6.

**Table 2**. Metrics report generated by Kriging interpolation

Metrics	Value
Count	1000
ME	-0.000000712
RMSE	0.014768321
MSE	0.00034932
RMSSE	1.009437264
ASE	0.014614952

ME - Mean Error, RMSE - Root Mean Square Error, MSE - Mean Standardized Error, RMSSE - Root Mean Square Standardized Error, ASE - Average Standard Error

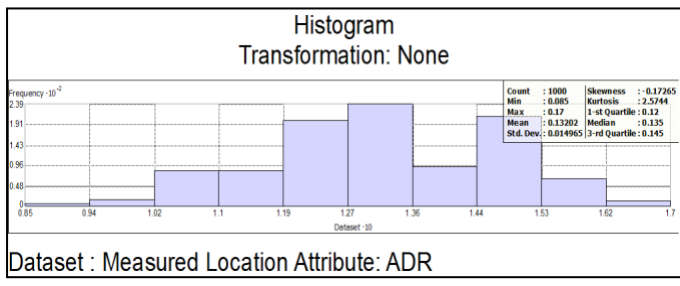


**Fig. 3.** Pre-validation of average gamma dose rates (ADR) distribution.

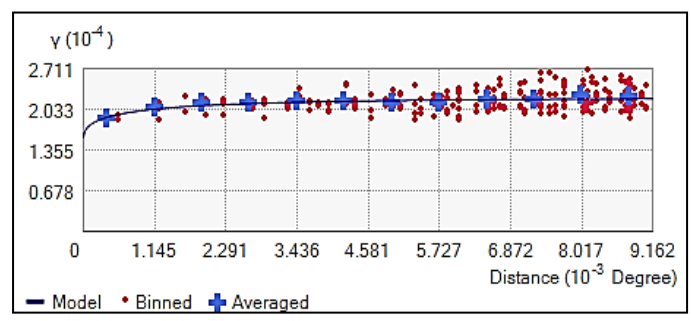


**Fig. 4.** Kriging semivariogram for spatial dependence analysis.

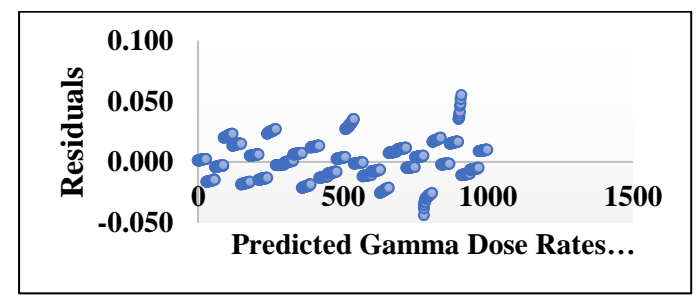


**Fig. 5.** Residual plot for post-validation of kriging model prediction accuracy.

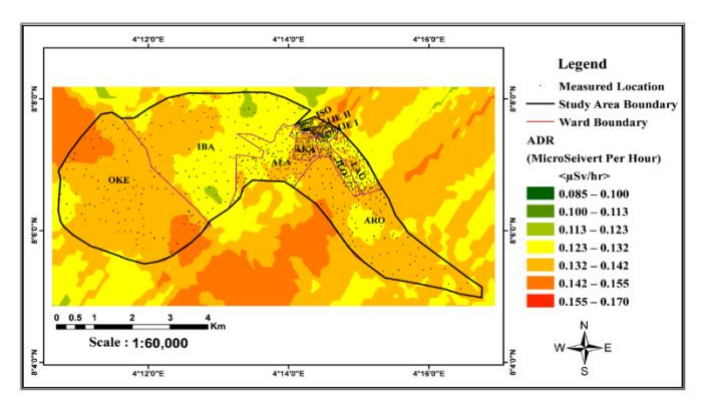


**Fig. 6.** Spatial map of predicted gamma dose rates within the study area

### 4. DISCUSSIONS

The average gamma dose rates (ADR) across the wards within the study area, as presented in Table 1, ranged from 0.122 to 0.139  $\mu$ Svh<sup>-1</sup>, with an overall average value of 0.132  $\mu$ Svh<sup>-1</sup>. This value is notably lower than the global average of 0.274  $\mu$ Svh<sup>-1</sup> [5] (Figure 7), indicating that natural background radiation is the dominant source in the region,

with minimal anthropogenic influence. However, while the ADR distribution appears relatively uniform, certain wards show notable differences. For instance, Oke-Ola (OKE) recorded the highest ADR at 0.139  $\mu Svh^{-1}$ , while Ijeru I (IJE I) had the lowest at 0.122  $\mu Svh^{-1}$ . These variations in ADR values can be attributed to differences in geological factors and soil characteristics across the wards, influencing the distribution and accumulation of naturally occurring radioactive materials (NORMs) [5,28].

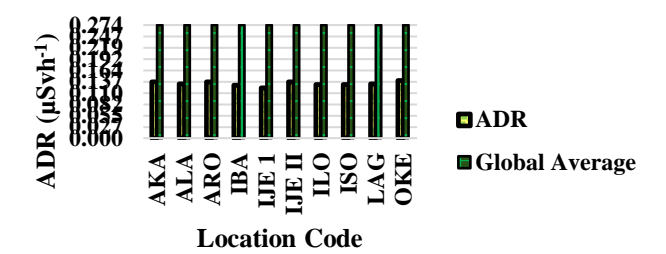


**Fig. 7.** Comparison of the ADR values measured with global average

Although the region generally shows limited anthropogenic influence, localized human activities such as artisanal mining, brick manufacturing, and agricultural practices which can disturb the soil and expose naturally occurring radioactive materials (NORMs), thereby elevating ADR levels in specific areas. In Oke-Ola, where crop cultivation is more prevalent, the higher radiation levels may reflect the disruption of soil and bedrock, leading to increased exposure to NORMs. Additionally, practices that contribute to soil erosion can further exacerbate this issue by transporting NORMs to the surface and redistributing them acre

Geological characteristics, particularly rock composition and soil type, significantly influence gamma radiation levels. Granite-rich areas tend to emit higher levels of gamma radiation due to the presence of NORMs like uranium, thorium, and potassium [5, 29]. In contrast, Ijeru I may feature less granite and more sedimentary soil types, which typically have lower concentrations of these radioactive elements. Additionally, soil composition influences radon gas retention; clay-rich soils, common in certain parts of Oke-Ola, tend to trap radon gas, leading to higher gamma radiation levels, whereas sandy soils, which may be more prevalent in Ijeru I, allow radon to disperse more easily. The geological structure of Oke-Ola, and clay-rich soil, may thus be a key factor contributing to its elevated ADR.

Furthermore, long-term environmental monitoring that focuses on factors such as soil moisture, land use changes, and seasonal variations in precipitation would enhance our understanding of how these conditions influence gamma radiation over time.

Table 3 compares the ADR findings from this study with previous research conducted in the study area and other regions. To maintain consistency, ADR values from earlier studies were converted to microSieverts per hour ( $\mu Svh^{-1}$ ). The highest ADR of  $0.156 \pm 0.03~\mu Svh^{-1}$  was reported by [33], potentially due to elevated terrestrial gamma radiation and significant human activities like mining and industrial development in that area. In contrast, the lowest ADR of  $0.019 \pm 0.00~\mu Svh^{-1}$  reported by [36] suggests significantly lower

radiation levels, likely resulting from less geological NORM presence and minimal anthropogenic impact.

**Table 3.** Comparison of this results obtained for ADR with those from other studies

Author	ADR Value (µSvh <sup>-1</sup> )
[29]	$0.037 \pm 0.00$
[30]	$0.067 \pm 0.00$
[31]	$0.133 \pm 0.00$
[32]	$0.120 \pm 0.00$
[33]	$0.156 \pm 0.03$
[34]	$0.039 \pm 0.00$
[35]	$0.132 \pm 0.02$
[36]	$0.019 \pm 0.00$
[37]	$0.052 \pm 0.00$
[38]	$0.098 \pm 0.00$
Present Study	$0.132 \pm 0.00$

The ADR value of  $0.132 \pm 0.00~\mu Svh^{-1}$  for Ogbomoso South Local Government, found in the present study, falls within this range and is higher than most except for those reported by [31] and [33] respectively. Differences in geological characteristics such as varying rock compositions, local mining activities, and agricultural practices are likely major factors influencing the disparity in radiation levels between these regions. This highlights the importance of continuous monitoring to ensure public health and safety, particularly in areas where human activities may increase.

Furthermore, the similarity between the ADR reported by [35] and the present study indicates consistency and reliability in the measurement methodologies, including the equipment and techniques used. This reinforces the accuracy of the findings and supports the conclusion that background ionizing radiation levels in Ogbomoso South Local Government, Oyo State, Nigeria, remain within internationally recognized safe limits. Continuous monitoring, particularly in areas with increased human intervention, will be essential to maintain these safety standards and address any future changes in radiation exposure.

The estimated annual effective dose equivalent (AEDE) shown in Table 1 ranges from 0.213 to 0.243 mSvy<sup>-1</sup>, with an average of 0.231 mSvy<sup>-1</sup>. This average remains below the recommended limit of 1 mSvy<sup>-1</sup> (Figure 8) for public exposure, as suggested by [39], indicating compliance with internationally accepted radiation standards. Similar AEDE values from prior research in the study area corroborate the low terrestrial gamma radiation levels emitted by radioactive materials. The highest AEDE was found in the Oke-Ola (OKE) ward at 0.243 mSvy<sup>-1</sup>, while the lowest was recorded in the Ijeru I (IJE I) ward at 0.213 mSvy<sup>-1</sup>. This pattern mirrors the ADR distribution, demonstrating a relatively uniform background radiation distribution.

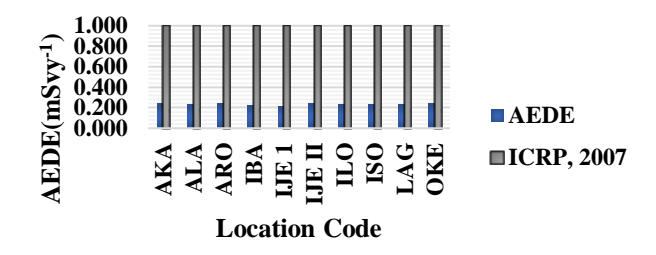


Fig. 8. Comparison of the estimated AEDE with ICRP limit.

The in-depth comparisons revealed that Ijeru I (IJE I) exhibited the lowest ADR (0.122 µSvh<sup>-1</sup>) and AEDE (0.213 mSvy<sup>-1</sup>), suggesting minimal NORM presence or industrial activity. Conversely, the Ibapon (IBA) ward showed slightly higher values, with an ADR of 0.128 μSvh<sup>-1</sup> and an AEDE of 0.224 mSvy<sup>-1</sup>, indicating marginally increased industrial activities. The wards Isoko (ISO) and Ilogbo (ILO) recorded equal ADR values of 0.130 μSvh<sup>-1</sup>, with AEDEs of 0.228 mSvy<sup>-1</sup> and 0.229 mSvy<sup>-1</sup>, respectively. The Lagbedu (LAG) and Alapata (ALA) wards reported ADRs of 0.131 μSvh<sup>-1</sup> and AEDEs of 0.230 mSvy<sup>-1</sup>. In contrast, Arowomole (ARO), Akata (AKA), and Ijeru II (IJE II) had higher ADR values of 0.136 µSvh<sup>-1</sup> and AEDEs ranging from 0.238 to 0.239 mSvy<sup>-1</sup>, indicating additional radiation sources. The Oke-Ola (OKE) ward, with the highest ADR of 0.139 µSvh<sup>-1</sup> and AEDE of 0.243 mSvy<sup>-1</sup>, suggests significant contributing factors to elevated radiation levels. Despite these variations, ADR and AEDE values remain within safe exposure limits, highlighting the need for continuous monitoring to identify and mitigate potential sources of increased radiation.

The pre-validation analysis of the gamma dose rates distribution at the measured locations, illustrated in Figure 3 revealed a skewness of -0.17265 and a kurtosis of 2.5744. The near-zero skewness indicates an approximately symmetric distribution, while the kurtosis value, slightly above 2, suggests a distribution that is close to normal but slightly platykurtic. These statistics confirm the normality and suitability for Kriging application.

The Kriging semivariogram for spatial dependence analysis, as shown in Figure 4, indicates strong spatial autocorrelation in the measured gamma dose rates, evidenced by the low nugget value, well-defined sill, and significant range. This spatial dependency is crucial for the Kriging model, ensuring that predictions at unobserved locations are based on meaningful spatial relationships. The identified range of spatial correlation supports the model's ability to accurately interpolate measured values, validating the appropriateness of using Kriging for this dataset.

The metric report generated by the Kriging interpolation and presented in Table 2, demonstrated that the model yields highly accurate predictions with minimal bias. Metrics such as mean error (ME), root mean square error (RMSE), and mean square error (MSE) are close to zero, while average standard error (ASE) values are reasonably close to RMSE. These low error metrics indicate that the predicted gamma dose rate values closely align with the actual measurements, enhancing confidence in the interpolated data. Additionally, the proximity of the root means squares standardized error (RMSSE) to 1 emphasizes the model's effectiveness in capturing the spatial variation of dose rates, further validating

the reliability of the interpolated gamma dose rate values derived from the Kriging model.

The residual plot in Figure 5, illustrating the differences between measured and predicted gamma dose rates, shows well-distributed residuals without obvious patterns. This distribution indicates that the model's predictions are unbiased and reliable; systematic deviations would have suggested issues with accuracy, but the absence of such patterns confirms the model's robustness.

The spatial map of predicted gamma dose rates, as presented in Figure 6, reveals an ADR range from 0.085 to 0.170 µSvh<sup>-1</sup>, exhibiting notable spatial heterogeneity. ADR values between 0.132 and 0.170 µSvh<sup>-1</sup> are predominantly measured in the eastern and western regions of the study area, particularly around the Oke-Ola (OKE) ward, where ADR levels exceed  $0.142~\mu Svh^{-1}$ , possibly due to geological formations or human activities. Conversely, the northern and southeastern parts, including the Ijeru I (IJE I) and parts of the Alapata (ALA), Ibapon (IBA), Lagbedu (LAG), Ilogbo (ILO), Arowomole (ARO), and Isoko (ISO) wards, exhibit lower ADR values between 0.085 and 0.123 µSvh<sup>-1</sup>, attributed to different soil compositions, vegetation cover, or reduced anthropogenic influences. The spatial map illustrates a gradient of relatively increasing ADR from the northwest to the southeast, reflecting transitions in the underlying factors affecting gamma radiation. The presence of several measured locations, indicated by black dots, provides a robust dataset for model validation, ensuring the reliability of the Kriging predictions

### 4.1 Limitations of the Kriging Model

While the Kriging model is a powerful tool for predicting gamma dose rates in unmeasured areas, certain limitations must be acknowledged. The accuracy of its predictions is heavily reliant on the density and distribution of measured data points. In regions with sparse data coverage, such as the northern and southeastern parts of the study area, the model may introduce interpolation errors, potentially underestimating or overestimating radiation levels. Studies have shown that increasing the number of measured locations significantly improves the accuracy of Kriging predictions [39]; therefore, future research should prioritize increasing the spatial density of sampling points to enhance model reliability.

Furthermore, the Kriging model assumes spatial continuity of radiation levels, which may not always hold true in areas experiencing abrupt geological or environmental changes. To address this limitation, future studies could explore hybrid models that combine Kriging with other geostatistical techniques, such as Co-Kriging or machine learning methods. These approaches could improve accuracy, especially in regions characterized by complex terrains or diverse land uses.

### 5. CONCLUSION

The application of the geostatistical kriging model in assessing exposure to background ionizing radiation and its radiological hazard indices in Ogbomoso South Local Government revealed that radiation levels are relatively low and within international safety limits, indicating no significant radiological hazard to the public. The findings show that the average gamma dose rate (ADR) and estimated annual

effective dose equivalent (AEDE) are 48.18% and 23.10% of the global averages and International Commission on permissible Radiological Protection (ICRP) respectively. This suggests a lower anticipated radiation exposure with minimal health risks. However, the ADR values, ranging between 0.132 and 0.170 µSvh-1, are primarily observed in the eastern and western regions of the study area, particularly around the "OKE" ward attributed to geological structure and clay-rich soil contributing to its elevated ADR. To ensure public safety, it is therefore recommended that a regular radiological monitoring program be established in Ogbomoso South Local Government. The data collected from this study can serve as a crucial baseline for future infrastructural developments which include industrial facilities, water systems, and energy plants. Additionally, increasing the number of sampling points in future studies will enhance the precision of spatial predictions, thereby reducing uncertainties in areas with sparse data coverage.

### REFERENCES

- [1] Environmental Protection Agency (2023). Radiation Protection: Radiation sources and doses. Retrieved from https://www.epa.gov/radiation/radiation-sources-and-doses#backgroundradiation.
- [2] Agency for Toxic Substances and Disease Registry. Toxicological Profile for Ionizing Radiation. Atlanta 1999, 438.
- [3] International Atomic Energy Agency. Environmental and Source Monitoring for Purposes of Radiation Protection. IAEA Safety Standards Series No. GSG-8. 2015.
- [4] World Health Organization. Ionizing radiation: sources and biological effects. Fact sheet no. 371, 2019. https://www.who.int/news-room/factsheets/detail/ionizing-radiation-health-effects.
- [5] UNSCEAR (2000). Sources and effects of ionizing radiation. United Nations Scientific Committee on the Effects of Atomic Radiation, UNSCEAR 2000 Report to the General Assembly, with Scientific Annexes, Volume I: Sources. United Nations, New York.
- [6] IAEA. (2013). Radiation Protection and Safety of Radiation Sources: International Basic Safety Standards. International Atomic Energy Agency.
- [7] M. O. Oviri, O. O. Fredrick and A. Ochuko. Environmental risk assessment of background radiation, natural radioactivity and toxic elements in rocks and soils of Nkalagu quarry, Southeastern Nigeria. Journal of Hazardous Materials Advances 2023, 10, 100288. https://doi.org/10.1016/j.hazadv.2023.100288
- [8] A. MbetAmos, U. Ibrahim, I. Shekwonyadu, O. J. Emmanuel, Y. Samson, and B. E. Godwin. Determination of natural radioactivity levels and radiological hazards in environmental samples from artisanal mining sites of Anka, North-West Nigeria. Scientific African, 2020, 10, e00561, https://doi.org/10.1016/j.sciaf.2020.e00561.
- [9] L. I. Nwankwo, D. F. Adeoti, and A. J. Folarin. Ionizing radiation measurements and assay of corresponding dose rate around bottling and pharmaceutical facilities in Ilorin, Nigeria. Journal of Science and Technology, 2014, 34(2), 84-92 http://dx.doi.org/10.4314/just.v34i2.10.
- [10] S. A. Bordner, D. A. Crosswell, A. O. Katz, and M. A. Ruderman. Measurement of background gamma radiation in the northern Marshall Islands. Reviewed by Makis Petratos and Ernst Sichtermann, 2016, 113 (25) 6833-6838.https://doi.org/10.1073/pnas.1605535113.
- [11] I. Guagliardi, G. Buttafuoco, C. Apollaro, A. Bloise, R. De Rosa, and D. Cicchella (2013). Using gamma-ray Spectrometry and Geostatistics for Assessing Geochemical Behaviour of Radioactive Elements in the Lese Catchment (southern Italy) Int. J. Environ. Res., 7(3):645-658.
- [12] C. Yeşilkanat, Y. Kobya, H. Taskin and U. Çevik. Dose rate estimates and spatial interpolation maps of outdoor gamma dose rate with geostatistical methods; A case study from Artvin, Turkey. Journal of Environmental Radioactivity. Ch 150 . 2015, 132-144 p. 10.1016/j.jenvrad.2015.08.011.

- [13] M. S. Rosenbaum and M. Söderström (1996). Geostatistics as an Aid to Mapping. Eleventh European Arc/Info User's Conference, London. Published on CD and Internet (http://www.esri.com/library/userconf/europroc96/PAPERS/PN11/PN11F.HTM).
- [14] X. Yao, B. Fu, Y. Lü, F. Sun, S. Wang, M. Liu. Comparison of Four Spatial Interpolation Methods for Estimating Soil Moisture in a Complex Terrain Catchment. PLoS ONE, 2013, 8(1): e54660. doi:10.1371/journal.pone.0054660
- [15] B. Usowicz, J. Lipiec, M. Łukowski, J Słominski. Improvement of Spatial Interpolation of Precipitation Distribution Using Cokriging Incorporating Rain-Gauge and Satellite (SMOS) Soil Moisture Data. Remote Sens. 2021, 13, 1039. https://doi.org/10.3390/rs13051039
- [16] D. V. Manthena, A. K. Ala, and A. Kumar. Interpolation of radon concentrations using GIS-based kriging and cokriging techniques Environmental Progress & Sustainable Energy, 2009 28 (4), 487-492. DOI 10.1002/ep.10407
- [17] W. Wu, X. P. Tang, X. Q. Ma et al. A comparison of spatial interpolation methods for soil temperature over a complex topographical region. Theor Appl Climatol, 2016, 125, 657–667. https://doi.org/ 10.1007/s00704-015-1531-x
- [18] D. E. Omosehinmi, A. M. Arogunjo. Geostatistical investigation and ambient radiation mapping of Akure north and south local government areas of Ondo state, Nigeria .IJSDR, 2016, 1(12)
- [19] H. T. Abba, M. G. Idris and J. S. Yaro. Mapping of Terrestrial Radioactivity Levels in Surface Soil. A Case Study of Damaturu L.G.A, Yobe State, Nigeria. Communication in Physical Sciences 2019, 4(2): 95-102. https://journalcps.com.
- [20] E. K. Chrisfanel, O. O. Jerry, A. O. Ibrahim, W. K. Raymond, E. Y. Ebenezer, N. Bawa, O. U. Aliyu and O. A. Millicent (2023). Geostatistical assessment of soils in Ibadan, Southwest Nigeria: Focus on agricultural lands, Environmental and Sustainability Indicators, 2023. DOI:10.1016/j.indic.2023.100287
- [21] P. C. Okoye and G. O. Avwiri. Evaluation of Background Ionizing Radiation Levels of Braithwaite Memorial Specialist Hospital Port Harcourt, River State. American Journal of Scientific and Industrial Research, 2013, 4(4): Pp 359 – 365.
- [22] O. U. Fredrick, and O. E. Eugene. Estimation of Annual Effective Dose and Excess Lifetime Cancer Risk from Background Ionizing Radiation Levels Within and Around Quarry Site in Okpoto-Ezillo, Ebonyi State, Nigeria. Journal of Environment and Earth Science. 2017, 7(12)
- [23] D. Turgay. The use of the GIS Kriging technique to determine the spatial changes of natural radionuclide concentrations in soil and forest cover. J Environ Health Sci Eng. 2014, 12: 130. doi: 10.1186/s40201-014-0130-6.
- [24] Z. Zhu, M. L. Stein. Spatial sampling design for prediction with estimated parameters. JABES, 2006 11, 24–44. https://doi.org/10.1198 /108571106X99751
- [25] N. Cressie, and K. W. Christopher. Statistics for Spatio-Temporal Data Wiley, 2011, 624 pp. Library of Congress Cataloguing-in-Publication Data 519.5—dc22 2010033576
- [26] E. Pebesma and R. Bivand. Spatial Data Science: With Applications in R (1st ed.). Chapman and Hall/CRC. 2023. https://doi.org/10.1201/ 9780429459016
- [27] R. M. Lark, D. J. Lapworth. Quality measures for soil surveys by lognormal Kriging, Geoderma, 2012, (173 – 174):231-240, https://doi.org/10.1016/j.geoderma.2011.12.008.https://www.sciencedire ct.com/science/article/pii/S0016706111003569.
- [28] J. Beretka and P. J. Mathew (1985). Natural radioactivity of Australian building materials, industrial wastes, and by-products. Health Physics Journal, 1985, 48(1), 87-95.
- [29] M. K. Akinloye, M. O. Ogunkinle, and O. P. Abodunrin (2007). Radiation exposure rates in the environment of Ogbomoso General Hospital. Science Focus, 12(2)152-156
- [30] O. O. Adewale, I. A. Tubosun, and J. O. Ojo (2015). Assessment Terrestrial Naturally Occurring Radioactive Material in soil and mine tailings in Awo and Ede, Osun-State, Southwest Nigeria. Ife Journal of Science. 2015, 17 (1), 199-209.
- [31] O. S. Ajayi, and S. B. Ibikunle (2013). Radioactivity of surface soils from Oyo state, South Western Nigeria. International Journal on Radiation Research., 2013, 11:4.

- [32] A. A. Essiett, I. E. Essien, and M. C. Bede (2015). Measurement of Surface Dose Rate of Nuclear Radiation in Coastal Areas of Akwa Ibom State, Nigeria. International Journal of Physics. 2015, 3 (5), 224-229.
- [33] J. C. Osimobi, E. O. Agbalagba, G. O. Avwiri, and C. P. Ononugbo (2015) GIS Mapping and Background Ionizing Radiation (BIR) Assessment of Solid Mineral Mining Sites in Enugu State, Nigeria. Open Access Library Journal. 2015, 2 (10), 1-9.
- [34] O. O. Oladapo, and E. A. Oni (2015). Activity Concentration of Gamma Emitting Natural Radionuclides in Building Materials. Elixir Nuclear & Radiation Physics. 2015, 86 35224-35226.
- [35] A. Alkasim, T. B. Muhammad, A. Ali, and G. Elvis (2017). Measurement of Gamma Radiation from Some Selected Refuse Dumpsites in Yola Metropolis, North – Eastern Nigeria. Journal of Applied Physics, 2017, 9(5), 13-17
- [36] G. A. Isola, O. M. Oni, M. K. Akinloye and P. S. Ayanlola (2018). Measurement of Natural Radioactivity in Soil Samples from Ladoke Akintola University of Technology, Ogbomoso South-West, Nigeria; International Journal of Scientific and Research Publications; 2018, 8(8);618–627. http://dx.doi.org/10.29322/IJSRP.8.8.2018.p8080.
- [37] P. O. Olagbaju, I. C. Okeyode, O. O. Alatise, B. S. Badab(2021). Background radiation level measurement using hand held dosimeter and gamma spectrometry in Ijebu-Ife, Ogun State Nigeria. International Journal of Radiation Research, 2021 19, No 3. http://dx.doi.org/ 10.18869/acadpub.ijrr.19.3.591.
- [38] E. A. Ajetunmobi, K. A. Shamsideen, O. C. Joseph, W. D. Timothy, R. O. Kolawole, T. T. Adetoro, E. B. Peter, and A. A. Sofiat (2023). In-situ measurements of dose rates in villages near mining sites in Oke-Ogun, Oyo state, Nigeria. Equity Journal of Science and Technology, 2023 10(1): 36 41.
- [39] ICRP (2007) The 2007 Recommendations of the International Commission on Radiological Protection. ICRP Publication 103. Annals of the ICRP, 2007, 37(2-4).